

## Thermal Stability of Zirconia as a Catalyst Support: Kinetics and Modelling

ALAIN MÉTHIVIER AND MICHÈLE PUJOLAT

*Département de Chimie-Physique des Processus Industriels, Ecole Nationale Supérieure des Mines,  
158 Cours Fauriel, 42023 Saint-Etienne Cedex 2, France*

Received January 22, 1992; revised July 8, 1992

The textural changes of two zirconium dioxide powders, one containing only tetragonal crystallites and the other a mixture of monoclinic and tetragonal crystallites, were investigated. The crystallite size increase was followed by means of X-ray diffraction line broadening for powders annealed in a controlled gaseous atmosphere at 600 and 770°C, in order to establish the variations of its experimental rate versus partial pressures of water and oxygen. An accelerating influence of water vapour was observed for both powders. A model, based on a catalytic effect of water vapour, and involving six elementary steps, was proposed in order to calculate theoretical rates within the approximation of the rate-limiting step. The comparison between the experimental and theoretical rate laws attests to the validity of the model and defines the most probable rate-limiting step: tetragonal crystallite growth proceeds at a rate controlled either by adsorption (or desorption) of water molecules or diffusion of hydroxyl groups; monoclinic crystallite growth is controlled by the diffusion of zirconium ions. © 1993 Academic Press, Inc.

### INTRODUCTION

Knowledge of the processes involved in thermal changes of catalyst supports is of great interest for the development of catalytic materials, as illustrated by various recent articles on the stability of transition alumina for postcombustion catalysis (1–3). During the last few years, the use of zirconia as a catalyst or catalyst support has been found very attractive for several reactions (4), including the production of hydrocarbons and (or) alcohols from CO and H<sub>2</sub> (5).

In our previous work on the thermal stability of  $\gamma$ -Al<sub>2</sub>O<sub>3</sub> and anatase TiO<sub>2</sub>, we have found evidence for a “catalytic” effect of water vapour on the surface area loss without phase transformation (6, 7). A model was proposed to explain the kinetics of surface area reduction in a gaseous atmosphere containing oxygen and water vapour. The diffusion of hydroxyl ions was found to be the rate-limiting step of the process for both oxides.

A particular feature of zirconia supports is that they very often contain two thermo-

dynamically stable crystallographic phases. It is known that tetragonal zirconia is “stabilized” with a small crystallite size due to its lower surface tension than in the monoclinic form and due to strain energy effects (8). At room temperature the tetragonal form is usually referred to as “metastable,” but from a thermodynamic point of view, it is really a stable phase. At high temperature, transformation into the monoclinic form may occur depending of the extent of growth.

In a recent study, Mercera *et al.* (9) have identified two processes for the loss in surface area of zirconia up to 850°C, namely, crystallite growth and neck growth between crystallites. These processes are accompanied by phase transformation of tetragonal into monoclinic crystallites. Due to this apparent complexity, the surface area will probably not properly reflect the overall modification. In this article, we report a detailed study of the influence of the gaseous atmosphere on the growth of tetragonal and monoclinic crystallites.

Several infrared spectroscopy studies

have reported that hydroxyl and carbonate species are present at the surface of zirconia powders (10–12). Moreover, it is known that zirconia is an oxygen-deficient oxide. Thus we have chosen to investigate only the influence of water vapour and oxygen, and in order to keep unchanged the content of surface carbonates on zirconia particles, the calcinations were carried out with a fixed partial pressure of carbon dioxide in the furnace atmosphere.

#### EXPERIMENTAL

##### *Samples*

A sample A of tetragonal zirconia with  $87 \text{ m}^2 \text{ g}^{-1}$  of initial surface area was prepared by Degussa. A sample B consisting of a mixture of tetragonal (30%) and monoclinic (70%) zirconia was obtained from hydrolysis of a solution of zirconium isopropylate in propanol. The gel was then dried in air for 3 h at  $120^\circ\text{C}$  and annealed for 4 h at  $450^\circ\text{C}$ . The resulting powder had an initial surface area of  $90 \text{ m}^2 \text{ g}^{-1}$ . The initial content in chloride was 0.3% (by weight).

##### *Surface Area Determination*

The specific surface area ( $S_{\text{BET}}$ ) of the initial and calcined powders was measured by the BET method using nitrogen adsorption at 77 K (Micromeritics 2100 E).

##### *X-ray Diffraction*

XRD spectra were recorded on a Siemens D501 diffractometer ( $\text{Cu } K\alpha$ ) which could be equipped with a high-temperature cell. The proportion of monoclinic and tetragonal phases was obtained by means of the intensity of the lines (111) for the tetragonal phase, (11 $\bar{1}$ ) and (111) for the monoclinic phase, using Adam and Cox's determination (13).

The mean crystallite size ( $\phi$ ) of the samples was calculated using X-ray line broadening analysis (14) according to Warren and Averbach's equation. The standard powder required by this method was prepared by annealing sample B for 12 h at  $1300^\circ\text{C}$  followed by slow cooling to room temperature.

Its mean crystallite diameter evaluated from the Debye–Scherrer method was 150 nm for both lines (111) and (11 $\bar{1}$ ) of the monoclinic form.

From this procedure the mean crystallite diameter obtained for sample A was 13.7 nm, and for sample B, 9.6 and 9.7 nm for the tetragonal and monoclinic phases, respectively. These are in agreement with the particle size which can be deduced from BET surface area determinations.

##### *Calcination*

The samples were calcined in a Pyrox B80 furnace equipped with an alumina tube and a West 2050 regulator. A thermocouple placed inside the alumina tube allowed the measurement of the temperature in the vicinity of the sample. The flowing gas was a mixture of argon, oxygen, and carbon dioxide at atmospheric pressure, the composition being adjusted by means of Brooks Shorate 150 flowmeters. The content in water vapour was fixed by flowing the previous mixture over a water bath whose temperature was regulated at the required value in the range  $-18^\circ/+15^\circ\text{C}$ . The partial pressure in oxygen and water vapour could be varied in the range 0.6–15.3 kPa and 0.13–2.1 kPa, respectively. That in carbon dioxide was arbitrarily maintained equal to 2.7 kPa. Prior to a calcination the furnace chamber was evacuated until 0.13 kPa, then the appropriate mixture was introduced. The time required to introduce the sample and establish the appropriate calcination conditions did not exceed 7 min. For the studies of the effects of  $\text{H}_2\text{O}$  and  $\text{O}_2$ , the temperature of calcination was fixed at  $770^\circ\text{C}$  for sample A, and at  $600^\circ\text{C}$  for sample B.

#### RESULTS

##### *Textural Changes*

The surface area of sample A after 2 h of calcination has been reported in Fig. 1a versus temperature. The dotted line corresponds to a calculated value ( $S_{\text{Cal}}$ ) of surface area which was obtained from the mean tetragonal crystallite diameter. The changes

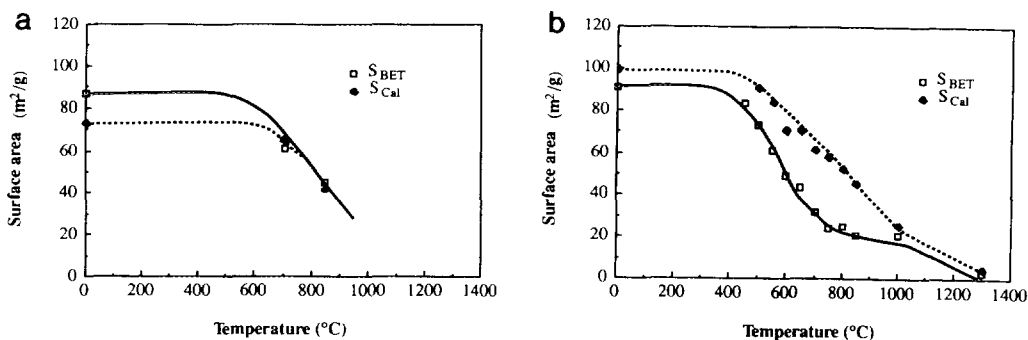


FIG. 1. Surface area of zirconia samples calcined for 2 h versus temperature: (a) sample A; (b) sample B.

in surface area obtained from the BET method ( $S_{\text{BET}}$ ) are identical to those of  $S_{\text{Cal}}$ , indicating that the surface loss is due to tetragonal crystallite growth. In consequence, the surface area as well as the crystallite diameter can be used to measure the extent of textural change in the case of tetragonal zirconia.

This is not the case for sample B, as can be seen in Fig. 1b. This reveals that the geometric surface ( $S_{\text{Cal}}$ ) corresponding to the crystallites takes, from 500 to 900°C, higher values than the surface area ( $S_{\text{BET}}$ ) which is accessible to gaseous molecules. This indicates that interfaces between crystallites have been formed which are not accessible to the gases, like grain boundaries, for example.

Furthermore, in the study of the effect of time at 770°C, it was observed that the major

part of tetragonal crystallites of sample A were not transformed into monoclinic ones, whereas their size increased until about 20.0 nm (15). In the case of sample B, the growth of the tetragonal and monoclinic crystallites was observed, but the amount of tetragonal phase decreased due to the tetragonal  $\rightarrow$  monoclinic transformation.

Finally, it was noted that the tetragonal  $\rightarrow$  monoclinic transformation could also occur during cooling the samples from the calcination temperature to room temperature, in agreement with Garvie's interpretations (8), due to the decreasing behavior of the critical diameter for this transformation versus temperature.

#### *Influence of Water Vapour and Oxygen*

Figure 2a shows the variations with time at 770°C of the mean crystallite diameter

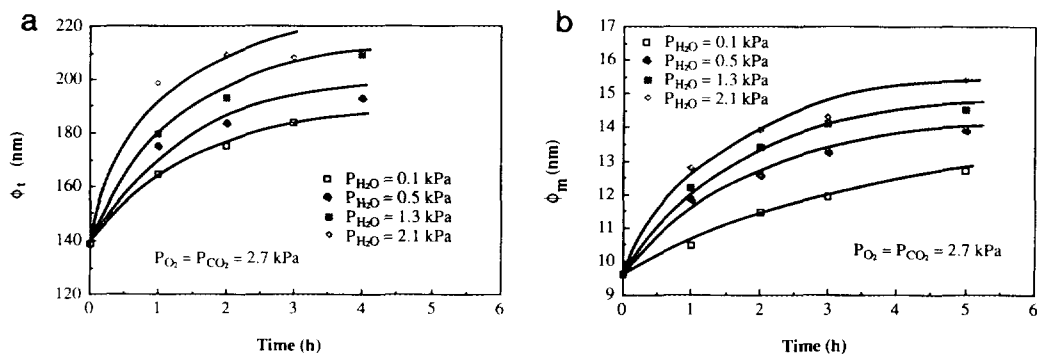


FIG. 2. Mean diameter of tetragonal crystallites versus time, influence of water vapour pressure: (a) sample A at 770°C; (b) sample B at 600°C.

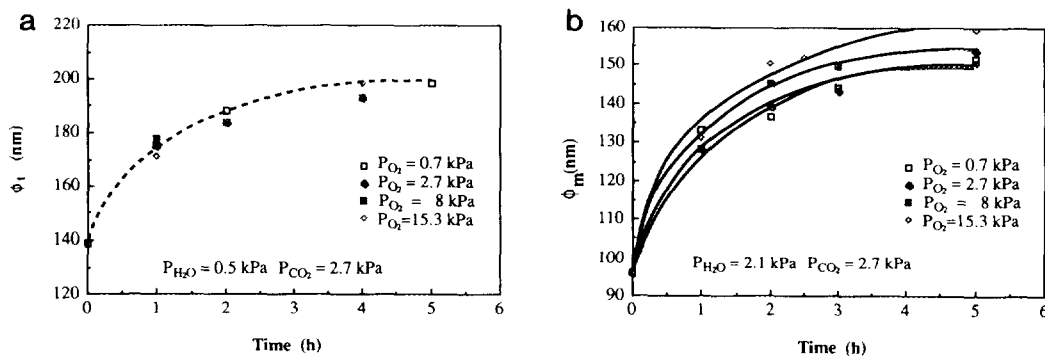


FIG. 3. Mean diameter of tetragonal crystallites of sample A versus time, influence of oxygen pressure: (a) sample A at 770°C; (b) sample B at 600°C.

of tetragonal crystallites of sample A for various partial pressures of water vapour. Water vapour was found to enhance tetragonal crystallite growth.

A similar change was obtained for sample B. This can be observed in Fig. 2b, which represents the variations of the mean crystallite diameter of monoclinic crystallites with time at 600°C, for several water vapour pressures. In the same way the influence of oxygen partial pressure could be obtained, and this is reported in Fig. 3a for sample A with a water vapour pressure equal to 0.5 kPa. No influence of oxygen can be observed. For sample B, the influence of oxygen is shown in Fig. 3b, where water vapour pressure was fixed at 2.1 kPa. It can be seen that in that case, oxygen slightly enhances the increase in mean monoclinic crystallite diameter. However, for lower water vapour pressures the influence of oxygen becomes hardly noticeable.

#### DISCUSSION

##### Textural Change

From the study of the two zirconia powders, it can be deduced that the growth of monoclinic crystallites in sample B may proceed via three parallel processes due to interactions between crystallites, as depicted in Scheme 1, in which contacts between monoclinic (m) and tetragonal (t) crystallites are represented.

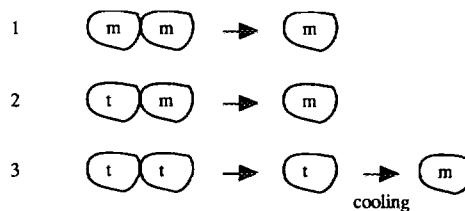
Each of these three interactions proceeds at a specific rate, denoted  $\mathcal{R}_1$ ,  $\mathcal{R}_2$ , and  $\mathcal{R}_3$ , which depends only on the chemical parameters (temperature, atmosphere). We have shown in a separate study (15) that the contribution of the second interaction to the growth of monoclinic crystallites is negligible. The overall rate of the process of monoclinic crystallite growth ( $d\phi_m/dt$ ) is thus given by

$$\frac{d\phi_m}{dt} = U\mathcal{R}_1 + W\mathcal{R}_3, \quad (1)$$

in which  $U$  and  $W$  are algebraic expressions that depend on physical constants and on the geometric arrangement of the powder (15).

For sample A which contains only tetragonal crystallites the rate of crystallite growth is given by

$$\frac{d\phi_t}{dt} = W\mathcal{R}_3. \quad (2)$$



SCHEME 1

The experimental curves reported in Figs. 2a, 2b, 3a, and 3b can be fitted using a mathematical function of time as

$$\phi = \phi_0(1 + At)^u, \quad (3)$$

where  $\phi$  is the mean crystallite diameter at time  $t$ ,  $\phi_0$  the initial mean crystallite diameter, and  $A$  and  $u$  are fitted parameters. In this way, the experimental kinetic rate of size increase ( $d\phi/dt$ ) can easily be deduced as a function of  $\phi$ , according to the following expression:

$$\frac{d\phi}{dt} = Au\phi_0 \left(\frac{\phi}{\phi_0}\right)^{u-1/u}. \quad (4)$$

In the case of a single interaction (Eq. (2)), for a given value of  $\phi$ , the rate is proportional to  $A$ , which represents the specific rate and depends only on the chemical variables (temperature, partial pressures, nature and amount of impurities, etc.). Thus the variations of the experimental rate  $d\phi/dt$ , for a fixed value of  $\phi$ , will lead to the expression of the specific rate versus partial pressures of water and oxygen, which can be easily compared to theoretical rate laws as deduced from models (6, 7). In the case of parallel interactions (Eq. (1)), in the mathematical function of Eq. (3),  $A$  has no physical meaning (15).

The values of  $\phi_i$  (sample A) and  $\phi_m$  (sample B), for which the rates have been determined, are 16.5 and 11.0 nm, respectively. Figures 4a and 4b represent the variations of  $(d\phi_i/dt)_{\phi_i=16.5}$  as a function of  $P_{H_2O}$  and  $P_{O_2}$  for sample A. The corresponding variations of  $(d\phi_m/dt)_{\phi_m=11.0}$  are given in Figs. 5a and 5b for sample B. It can be seen that for both samples the enhancing influence of water vapour is rather strong. The influence of oxygen is nearly negligible; a slight increasing effect can be noticed for sample B when the water vapour pressure takes values higher than 1.3 kPa.

#### A Model for Crystallite Growth

As in the case of anatase and alumina (6, 7), the textural changes of zirconia are found

to be strongly enhanced by water vapour. This is in good agreement with the results of Murase and Kats (16) and Villa Garcia *et al.* (17). Moreover, the zirconia surface exhibits hydroxyl groups until 700°C, as revealed by infrared spectroscopy (10, 11), which are the result of the dissociation of water molecules at the surface. These species will be considered as surface point defects, denoted  $\text{OH}_O^\cdot$  according to Kröger notation. As with anatase, zirconia is known to be an oxygen-deficient oxide; one may assume it contains oxygen vacancies, denoted  $\text{V}_O^{\cdot\cdot}$ . For these reasons, we have chosen to describe the crystallite growth of zirconia by means of the model based on a "catalytic" effect of water vapour, as previously reported for titania and transition alumina (6, 7). This model is based on the description, on the atomic scale, of the transport of the structural elements of the oxide ( $\text{Zr}_{Zr}^\vee$  and  $2\text{O}_O^\ominus$ ) from surfaces of positive curvature radii (denoted  $R > 0$ ) towards surfaces of negative curvature radii (denoted  $R < 0$ ). These latter surfaces correspond precisely to the neck between two crystallites. Six elementary steps given in Table 1 are proposed in order to take into account the observed influence of water vapour.

In this model it may be noted that water vapour plays a crucial role through the diffusion of hydroxyl ions.

#### Theoretical Rates Calculated from the Model

The resolution of the kinetic model proposed in Table 2 may be easily achieved with the aid of the following assumptions:

- the kinetic rates are evaluated according to the method of the rate-limiting step;
- the diffusion steps are evaluated according to Fick's first law within Wagner's approximation (constant concentration gradient);
- the concentration of some crystal imperfections involved in the reactions of Table 1 can be calculated in a simple manner

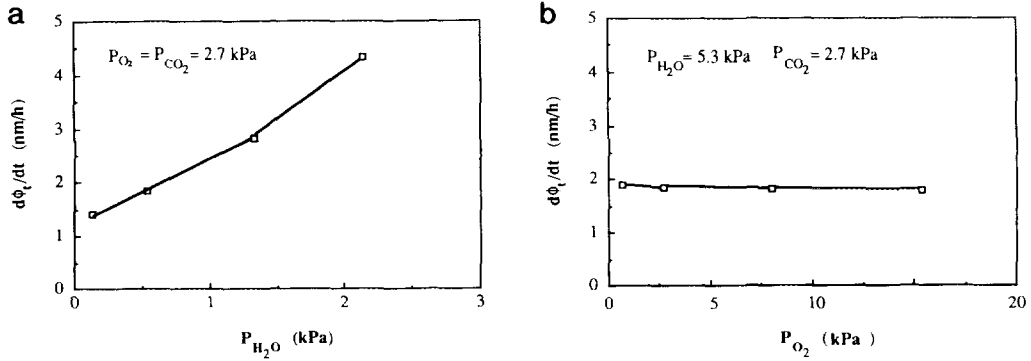


FIG. 4. Rate of tetragonal crystallite growth (for  $\phi_t = 16.5$  nm) in sample A at 770°C versus (a) water vapour pressure and (b) oxygen pressure.

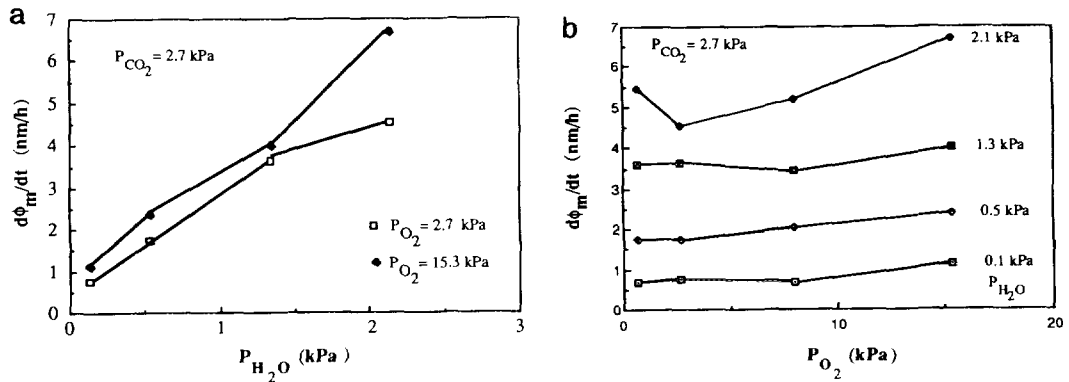


FIG. 5. Rate of monoclinic crystallite growth (for  $\phi_m = 11.0$  nm) in sample B at 600°C versus (a) water vapour pressure and (b) oxygen pressure.

TABLE I

Elementary Steps for the Model of Crystallite Growth in  $ZrO_2$

Elementary step	Quasi-chemical reaction
1. Water adsorption at $R > 0$ surfaces	$H_2O_g + O_{O_{R>0}}^x + V_{O_{R>0}}^{\bullet\bullet} = 2 OH_{O_{R>0}}^{\bullet}$
2. Hydroxyl diffusion	$OH_{O_{R>0}}^{\bullet} \rightarrow OH_{O_{R<0}}^{\bullet}$ (and $V_{O_{R<0}}^{\bullet\bullet} \rightarrow V_{O_{R>0}}^{\bullet\bullet}$ )
3. Vacancy creation at $R < 0$ surfaces	$2 OH_{O_{R<0}}^{\bullet} + 2 OH_{O_{R<0}}^{\bullet} = 4 OH_{O_{R<0}}^{\bullet} + V_{Zr_{R<0}}^{\bullet\bullet\bullet\bullet} + 2 V_{O_{R<0}}^{\bullet\bullet}$
4. Water desorption at $R < 0$ surfaces	$2 OH_{O_{R<0}}^{\bullet} = H_2O_g + O_{O_{R<0}}^x + V_{O_{R<0}}^{\bullet\bullet}$
5. Zirconium diffusion	$V_{Zr_{R<0}}^{\bullet\bullet\bullet\bullet} \rightarrow V_{Zr_{R>0}}^{\bullet\bullet\bullet\bullet}$ (and $Zr_{Zr_{R>0}}^x \rightarrow Zr_{Zr_{R<0}}^x$ )
6. Vacancy annihilation at $R > 0$ surfaces	$V_{Zr_{R>0}}^{\bullet\bullet\bullet\bullet} + 2 V_{O_{R>0}}^{\bullet\bullet} = 0$

Note. Kröger notation is used.

TABLE 2

Expression of the Rate Deduced from the Model of ZrO<sub>2</sub> Crystallite Growth

Rate-limiting step	[OH <sub>0</sub> ] ≫ [V <sub>0</sub> ]	[V <sub>0</sub> ] ≫ [OH <sub>0</sub> ]
1.	$k_1 K^1 P_{H_2O}^2 P_{O_2}^{-1/4}$	$4^{-5/6} k_1 K^{1/3} P_{H_2O} P_{O_2}^{-1/6}$
2.	$k_2 (K K_1)^{1/4} P_{H_2O}^4 P_{O_2}^{-1/8}$	$4^{-7/6} k_2 K^{1/6} K_1^{1/2} P_{H_2O}^2 P_{O_2}^{-1/12}$
3.	$k_3 K K_1 P_{H_2O} P_{O_2}^{-1/2}$	$4^{-2/3} k_3 K^{2/3} K_1^{1/3} P_{H_2O} P_{O_2}^{-1/6}$
4.	$k_4 (K K_1)^{1/2} P_{H_2O}^2 P_{O_2}^{-1/4}$	$4^{-5/6} k_4 K^{1/3} K_1 P_{H_2O} P_{O_2}^{-1/6}$
5.	$k_5 K_3 (K K_1)^{-1} K_4^{-2} P_{H_2O} P_{O_2}^{1/2}$	$4^{2/3} k_5 K_3 K_4^{-1/2} K_4^{-2/3} P_{O_2}^{1/3}$
6.	$k_6 K_3 (K_1 K_4)^{-2}$	$k_6 K_3 (K_1 K_4)^{-2}$

Note.  $k_i (1 \leq i \leq 6)$  is the rate constant relative to the *i*th step,  $K_i (1 \leq i \leq 6)$  is the equilibrium constant relative to the *i*th step, and  $K$  is the equilibrium constant between zirconia and oxygen.

by using Brouwer's approximation (18) in the equation of charge balance of the crystal, which takes the following form (*e* is the concentration of electrons):

$$[OH_0] + 2[V_0] = e + 4[V_{Zr}'] \quad (5)$$

As the term  $4[V_{Zr}']$  may be neglected, two limiting conditions have to be considered:  $[OH_0] \gg [V_0]$  and  $[OH_0] \ll [V_0]$ .

— zirconia is supposed to be at equilibrium with gaseous oxygen according to

$$O_0 = \frac{1}{2} O_2 + V_0 + 2e' \quad (6)$$

The calculation of the rate law leads to the following general expression, as previously reported (6, 7):

$$r = k P_{H_2O}^\alpha P_{O_2}^\beta \quad (7)$$

The various determinations of *k*,  $\alpha$ , and  $\beta$  are reported in Table 2 for each assumed rate-limiting step and each limiting condition of the charge balance equation (5).

*Comparison between Experimental and Calculated Rates*

Let us first discuss the results obtained with sample A, for which crystallite growth results from the single interaction between tetragonal crystallites. Among the possible

expressions of the rate law reported in Table 2, we have selected those which exhibit an accelerating influence of water vapour, in order to be in agreement with the experimental results (cf. Figs. 2a and 4a). Then we have confronted the experimental results of the rate for  $\phi$  equal to 11.5 nm to these theoretical rate laws. The best agreements were obtained with the two following expressions:  $P_{H_2O} P_{O_2}^{-1/6}$  and  $P_{H_2O}^{1/2} P_{O_2}^{-1/12}$ . It is difficult to choose between these two expressions to decide which of them corresponds to the rate-limiting step: either the steps of adsorption (or desorption) of water molecules, or the step of hydroxyl diffusion are equally possible (steps 1 or 4, or 2 of Table 2, respectively). For each of them, the predominant point defects in Eq. (5) are oxygen vacancies and electrons.

In the case of sample B, we have previously seen that the growth of monoclinic crystallites could result from two distinct interactions. Consequently the rate of monoclinic crystallite growth, which may be expressed by the sum of two terms (cf. Eq. (1)), takes the form

$$\left(\frac{d\phi_m}{dt}\right)_{\phi_m=ct} = a_1 P_{H_2O}^{\alpha_1} P_{O_2}^{\beta_1} + a_3 P_{H_2O}^{\alpha_3} P_{O_2}^{\beta_3} \quad (8)$$

in which  $a_1, \alpha_1, \beta_1, a_3, \alpha_3$ , and  $\beta_3$  have to be determined in order to fit the experimental rates.

The best agreement that could be found, for a value of  $\phi_m$  equal to 11.0 nm, was obtained for the two equations

$$\left(\frac{d\phi_m}{dt}\right)_{\phi_m=ct} = a_1 P_{H_2O} P_{O_2}^{1/2} + a_3 P_{H_2O}^{1/2} P_{O_2}^{-1/12} \quad (a_1 = 0.667, a_3 = 1.462) \quad (9)$$

$$\left(\frac{d\phi_m}{dt}\right)_{\phi_m=ct} = a_1 P_{H_2O} P_{O_2}^{1/2} + a_3 P_{H_2O}^{1/2} P_{O_2}^{-1/4} \quad (a_1 = 0.761, a_3 = 1.190). \quad (10)$$

However, it is not possible to decide which of them gives the best agreement, so both are equally possible for explaining the textural changes of sample B.

Further interpretation can be obtained by considering all the possible expressions obtained for the two samples A and B (15). It appears that the expression  $P_{\text{H}_2\text{O}}^{1/2} P_{\text{O}_2}^{-1/2}$  is the most probable rate law for the tetragonal crystallite growth of sample A, which corresponds to the diffusion of hydroxyl groups as the rate-limiting step. This leads to the attribution of the expression  $P_{\text{H}_2\text{O}} P_{\text{O}_2}^{1/2}$  to the interaction between monoclinic crystallites. This corresponds, as can be seen in Table 2, to the diffusion of zirconium ions as the rate-limiting step. This also shows that predominant point defects in monoclinic zirconia should be hydroxyl ions and electrons (cf. Table 2, second column and fifth row).

It may be emphasized that our kinetic study leads to the same mechanism for both monoclinic and tetragonal particles, but with distinct rate-limiting steps and distinct predominant point defects. In the monoclinic phase, zirconium diffusion is rate-limiting, whereas in the tetragonal phase, either adsorption (or desorption) of water molecules or hydroxyl diffusion can be rate-limiting. The fact that hydroxyl ions are predominant over oxygen vacancies at the surface of monoclinic particles, and that the opposite case occurs with tetragonal particles, is a result of the quantitative modelling. Infrared studies of monoclinic and tetragonal zirconia have shown spectral differences that can be attributed to the differences in surface sites (11, 19). To our knowledge, no experiments are actually available to verify our conclusions, but it can be proposed that such a difference may be a consequence of a better stability of hydroxyl groups in the case of monoclinic crystallites. Within such a description, tetragonal surfaces would preferentially exhibit oxygen vacancies, that correspond to the so-called Lewis-acid sites (unsaturated zirconium ions).

Finally, water vapour enhances surface area decrease by crystallite growth in both tetragonal and monoclinic zirconia, whereas oxygen inhibits that of tetragonal crystallites and enhances that of monoclinic ones.

## CONCLUSIONS

The textural changes of a tetragonal zirconia powder can be followed either by the surface area decrease or the crystallite growth. Those of zirconia containing both tetragonal and monoclinic crystallites proceed via two processes: crystallite growth (either monoclinic or tetragonal) and interface growth between crystallites. The surface area is not suitable for determining the rate of thermal evolution of two-phased zirconia powders. The rate of monoclinic crystallite growth is much more appropriate.

The experimental variations of the kinetic rate of crystallite growth versus partial pressures in water and oxygen have been reported for both monoclinic and tetragonal zirconia. Water vapour has been found to accelerate crystallite growth in both polymorphs.

An attempt has been made to interpret these results quantitatively according to a model based on a "catalytic" effect of water vapour. This showed that:

— for tetragonal crystallite growth, the rate-limiting step was found to be either the adsorption (or desorption) of water, or the diffusion of hydroxyl groups.

— for monoclinic crystallite growth, the rate is given by a sum of two terms that correspond to (i) the interaction between monoclinic crystallites and (ii) the interaction between tetragonal crystallites, providing a tetragonal crystallite which transforms to a monoclinic one by subsequent cooling to room temperature. Both phenomena are accelerated by water vapour. The rate-limiting step for the interaction between monoclinic crystallites is zirconium diffusion.

This study shows also how quantitative modelling associated with an appropriate kinetic study may lead to the validation of a model, in which all the elementary steps of a process are taken into account. However, it has not been possible to decide without any doubt between two rate-limiting steps in the case of tetragonal zirconia. This particular result is useful to point out the limits



of the method, as well as the necessity of a detailed kinetic study before concluding about mechanisms and rate-limiting steps.

Finally, the agreement between experiments and model suggests that predominant charged defects are not of the same kind for monoclinic and tetragonal zirconia surfaces, which could be useful for the comprehension of their catalytic properties.

#### ACKNOWLEDGMENTS

Financial support for this study has been provided by the Institut Français du Pétrole (Rueil-Malmaison). The authors gratefully acknowledge Dr. P. Chaumette and Dr. G. Mabilon for their collaboration. Dr. V. Perrichon from the Institut de Recherches sur la Catalyse, CNRS (Villeurbanne) is gratefully acknowledged for providing (single-phased) tetragonal zirconia powder. The authors warmly acknowledge Professor M. Soustelle (E.N.S.M., Saint-Etienne) for helpful discussions.

#### REFERENCES

- Oudet, F., Courtine, P., and Vejux, A., *J. Catal.* **114**, 112 (1988).
- Burtin, P., Brunelle, J. P., Pijolat, M., and Soustelle, M., *Appl. Catal.* **34**, 225 (1987).
- Beguín, B., Garbowski, E., and Primet, M., *J. Catal.* **127**, 595 (1991).
- Tanabe, K., *Mater. Chem. Phys.* **13**, 347 (1985).
- Silver, R. G., Hou, C. J., and Ekerdt, J. G., *J. Catal.* **118**, 400 (1989).
- Hébrard, J. L., Pijolat, M., and Soustelle, M., *J. Am. Ceram. Soc.* **73**, 79 (1990).
- Pijolat, M., Dauzat, M., and Soustelle, M., *Solid State Ionics* **50**, 31 (1992).
- Garvie, R. C., *J. Phys. Chem.* **82**, 218 (1978).
- Mercera, P. D. L., van Ommen, J. G., Doesburg, E. B. M., Burggraaf, A. J., and Ross, J. R. H., *Appl. Catal.* **57**, 127 (1990).
- Fuller, E. L., Holmes, H. F., Jr., and Gammage, R. B., *J. Colloid Interface Sci.* **33**, 623 (1970).
- Agron, P. A., Fuller, E. L., and Holmes, H. F., Jr., *J. Colloid Interface Sci.* **52**, 553 (1975).
- Morterra, C., and Orío, L., *Mater. Chem. Phys.* **24**, 247 (1990).
- Adam, J., and Cox, B., *J. Nucl. Energy, Part A* **11**, 31 (1959).
- Guinier, A., in "Théorie et Technique de la Radiocristallographie," 3ème éd., p. 461. Dunod, Paris, 1964.
- Méthivier, A., Thesis, 1992. Saint-Etienne, France.
- Murase, Y., and Kato, E., *J. Am. Ceram. Soc.* **66**, 196 (1982).
- Villa Garcia, M. A., Trobajo Fernandez, M. C., and Otero Areán, C., *Thermochim. Acta* **126**, 33 (1988).
- Brouwer, G., *Philips Res. Rep.* **9**, 366 (1954).
- Hertl, W., *Langmuir* **5**, 96 (1989).